Cloud-to-Ground Lightning throughout the Lifetime of a Severe Storm System in Oklahoma

MARK A. SHAFER*

School of Meteorology, University of Oklahoma, Norman, Oklahoma

DONALD R. MACGORMAN

National Severe Storms Laboratory, Norman, Oklahoma

FREDERICK H. CARR

School of Meteorology, University of Oklahoma, Norman, Oklahoma

(Manuscript received 8 February 1999, in final form 9 August 1999)

ABSTRACT

Cloud-to-ground (CG) lightning data are examined relative to digitized radar data for a storm system that occurred in Oklahoma on 26 May 1985. This system evolved through three stages: 1) two lines of cells, one near the dryline and the other 60 km ahead of it; 2) a supercell storm; and 3) a mesoscale convective system (MCS). The behavior of lightning in each stage was different. Initially no ground flashes were observed in either line until reflectivity increased to $\geq$46 dBZ and vertically integrated liquid (VIL) increased to $\geq$10 kg m^{-2}; then ground flash rates remained $<$1.2 min^{-1} for $>$1 h. Most ground flashes in the line of storms near the dryline were negative (18 $-$CG, 3 $+$CG), while most in the leading line were positive (11 $+$CG, 3 $-$CG), a pattern of polarity opposite to what usually has been observed. Approximately 3 h after radar detected the first storm, ground flash rates increased to $>$5 min^{-1} and remained so for 6 h. A mesocyclone formed approximately 30 min after flash rates exceeded 5 min^{-1}, and a few positive ground flashes occurred near it. Ground flash rates increased briefly to $>$20 min^{-1} as the mesocyclone dissipated and then remained $>$10 min^{-1} as a squall line formed along the outflow boundary from the dissipating supercell and produced a stratiform region. Most ground flashes in this MCS occurred in the convective line and had negative polarity. The few ground flashes in the stratiform region tended to be positive (42 $+$CG, 32 $-$CG during 3 h). During 1 h of the MCS, ground flash rates decreased and then increased again simultaneously in both the convective and stratiform regions, a previously undocumented behavior. It is possible that this was caused by updrafts in both the convective line and stratiform region changing at roughly the same time. It is also possible that most ground flashes in the stratiform region originated near the convective line, and so were influenced by the line. Overall trends in ground flash density, flash relative frequency, reflectivity, VIL, and severe hail reports appeared similar as the storm system evolved.

1. Introduction

This study examines the polarity, flash rates, and flash density of cloud-to-ground flashes relative to severe weather and other storm characteristics in a system of storms that occurred in Oklahoma on 26 May 1985, during the Preliminary Research Experiment for Stormscale Operational and Research Meteorology (PRE-STORM) field program. This case was chosen because the storm system produced large hail (diameter greater than 1.9 cm, ¾ in.), a mesocyclone, and many ground flashes that lowered positive charge to ground ($+$CG flashes), as well as the more common ground flashes that lowered negative charge to ground ($-$CG flashes). Furthermore, the case included a variety of storm types as it evolved, beginning with low-precipitation storms near a dryline, then forming a supercell storm, and eventually becoming a mesoscale convective system. The evolution of ground flash polarity in the storm system of 26 May had characteristics that have not been documented previously. Thus, this paper discusses the behavior of ground flashes in the various stages of the storm system, along with the behavior of ground flashes in the vicinity of the mesocyclone.

* Current affiliation: Oklahoma Climatological Survey, Norman, Oklahoma.

Corresponding author address: Mark Shafer, Oklahoma Climatological Survey, 100 E. Boyd, Suite 1210, Norman, OK 73019-1012. E-mail: mshafer@ou.edu

a. Previous studies of cloud-to-ground lightning data

National Weather Service (NWS) offices now have access to cloud-to-ground lightning data from the U.S. National Lightning Detection Network (described by Cummins et al. 1998), but most applications of these data in the NWS have been fairly straightforward. Examples of present applications include using the national ground strike data to identify the existence, coverage, configuration, growth, dissipation, and motion of thunderstorms. Little has been done to use lightning data with radar or satellite data in more sophisticated ways to improve capabilities to infer other thunderstorm properties. This is partly because knowledge of the underlying relationships needed to support more sophisticated applications is still embryonic. Although some studies have identified promising relationships, not enough cases have been analyzed to determine how generally the relationships are valid or, alternatively, under what conditions they are valid.

For example, several studies have examined lightning ground flash rates relative to the occurrence of tornadoes [e.g., see Perez et al. (1997) and review by MacGorman (1993)]. Often ground flash rates reach a minimum when a tornado occurs and when the parent mesocyclone intensifies; then rates increase as the mesocyclone dissipates. Sometimes, however, ground flash rates peak during tornadoes. MacGorman and Nielsen (1991) hypothesized that ground flash rates are small during mesocyclones having an updraft capable of creating a pronounced weak echo region through much of the vertical depth of the storm, and that they peak during mesocyclones having weaker or shallower updrafts. In both cases, +CG flashes sometimes begin to occur in clusters around the mesocyclone as it forms. MacGorman and Nielsen's hypothesis has not yet been tested adequately, and there has not yet been a systematic study of conditions under which +CG flashes occur with mesocyclones.

Another example is an apparent association between +CG flashes and large hail. Such a relationship began to be reported anecdotally shortly after the capability of detecting +CG flashes was added to lightning locating systems. Later, a climatological study by Reap and MacGorman (1989) found that the probability of severe weather, particularly large hail, increased as +CG flash density increased, although not as −CG flash density increased. Subsequently, MacGorman and Burgess (1994) studied 15 severe storms in which the majority of ground flashes were positive during some period of at least 30 min and found that large hail tended to occur during periods when +CG flashes dominated ground flash activity.

Carey and Rutledge (1998) compared +CG flash occurrence with the fall of large hail inferred from multiparameter radar data for one storm and found that +CG flashes began as hail descended, but that the flashes continued after all large hail had reached the ground.

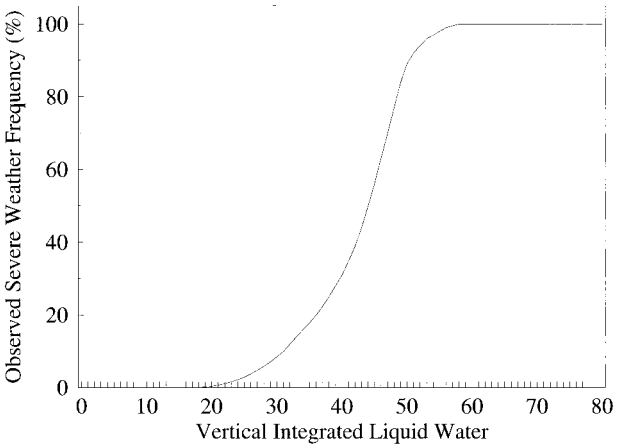

FIG. 1. Frequency of severe weather occurrence vs VIL during 1982 (from Devore 1983).

Thus, they suggested that the charge involved in the positive ground flashes was not carried by large hail, but was carried on smaller particles down through middle levels of the storm by the downdraft that formed as hail began to fall. Additional studies are needed to understand and further test apparent relationships between +CG flashes, large hail, and storm kinematics in storms dominated by +CG flashes for some period and to examine whether similar relationships exist when +CG flashes occur in storms always dominated by −CG flashes.

b. Relationship between VIL and severe weather

Though vertically integrated liquid (VIL) does not provide as much information about hail occurrence as the multiparameter radar data used by Carey and Rutledge (1998), high VIL values have shown a strong correlation to the occurrence of large hail in storms on the Great Plains (e.g., Saffle 1977; Elvander 1980; Devore 1983). Using a climatological study of springtime storms across Oklahoma, Devore (1983) examined the probability of a storm producing large hail as a function of its maximum VIL value. He found that storms with VIL values of less than 40 kg m^{-2} usually did not produce large hail, but storms with VIL values of 60 kg m^{-2} or greater almost always did (Fig. 1).

VIL in combination with other parameters provides additional improvements to the process of detecting large hail. Saffle and Elvander (1981) combined VIL data with other digitized radar products to produce a Severe Weather Probability (SWP) algorithm. Jackson and Crawford (1988) extended Saffle and Elvander's work by combining digitized radar data with products derived from data collected by a network of surface stations during the PRE-STORM project. The equations they developed again indicated the importance of VIL as a predictor.

In a test of the utility of digitized radar data products,

McGovern et al. (1984) showed a dramatic increase in severe storm warning capabilities from previous years. Using the contingency table developed by Devore, they improved the probability of detection for severe thunderstorms in Oklahoma over previous years, while decreasing the false alarm ratio dramatically. Furthermore, the area covered by warnings decreased, making warnings not only more accurate, but more precise in location. The warning improvement was most notable during springtime storms. This seasonal variation in performance was attributed to the SWP algorithm having been derived using early springtime storms in Oklahoma.

2. Instrumentation

The data used in this study come from the PRE-STORM field project, which operated during May–June 1985 across Oklahoma and Kansas. One of the goals of PRE-STORM was to test the use of new data systems, including wind profilers and a lightning detection system, in studies of mesoscale convective systems. Other data systems included a large network of closely spaced surface stations across Oklahoma and Kansas, Doppler radars in central Oklahoma and south-central Kansas, and supplemental soundings at nonstandard times for both established and temporary sites. Our analysis focuses on ground flash data and digitized Weather Surveilance Radar-1957 (WSR-57) data from Oklahoma City for the storm system that occurred in Oklahoma on 26 May 1985.

a. Digitized radar data

Data from the WSR-57 radar (10-cm wavelength, 2° half-power beamwidth) at Oklahoma City were used to produce a variety of horizontal and vertical cross sections of storm structure for this study. The Radar Data Processor II (RADAP II) system (McGrew 1972) automatically processed real-time digital radar data to produce products to help visualize areas of greatest severe weather threat [updated versions of many RADAP II products were subsequently included in the suite of products for the Weather Surveillance Radar-1988 Doppler (WSR-88D)]. The system used azimuthal scans at an automated sequence of elevation angles to sample a volume, each sequence requiring roughly 10 min. The elevation of successive scans was incremented 2° from the base scan to 22° or until no more echoes were detected.

Reflectivity data from each elevation angle were converted by a minicomputer into 15 RADAP II precipitation intensity levels. Reflectivity values were used to derive four classes of products: zero-tilt reflectivity (ZTR), volumetric products, accumulated rainfall, and severe weather. ZTR values were coded by using the standard NWS scale of digital video integrator and processor (VIP) levels, shown in Table 1. Volumetric data included echo tops and VIL. Severe weather products included storm motion, weak echo regions, and severe weather probability indices.

TABLE 1. Reflectivity and rainfall rates by VIP level.

VIP level	Reflectivity*	Rainfall rate**
1	18–29	0.02–0.09
2	30–40	0.10–0.49
3	41–45	0.50–0.99
4	46–49	1.00–1.99
5	50–56	2.00–4.99
6	≥57	≥5.00

* Radar reflectivity in dBZ.
** Calculated rainfall rate in in. h^{-1}.

VIL is the vertical integration, above a particular x–y location, of reflectivity values that have been converted to mass of liquid water. The RADAP II system calculated VIL on a 5 km × 8 km grid by using

$$\text{VIL} = \sum_{i=1}^{n-1} 3.44 \times 10^{-6} \frac{(Z_i + Z_{i+1})(h_{i+1} - h_i)}{2},$$

where Z_i is the reflectivity measured in $\text{mm}^6\ \text{m}^{-3}$, i is the sequence number of elevation scans, n is the total number of elevation scans, and h_i is the height of the ith scan at the x–y location being evaluated. The multiplication factor represents a conversion from reflectivity to liquid water by using an assumed exponential drop-size distribution (Greene and Clark 1972). VIL is related to precipitable water, which can be obtained by dividing VIL by the density of water.

b. Ground flash data

The ground flash data for this study were provided by a network of direction finders (DFs) manufactured by Lightning Location and Protection, Inc., (now Global Atmospherics, Inc.) and operated by the National Severe Storms Laboratory (NSSL). A map of the direction-finder stations is shown in Fig. 2. Each station in the network determined the direction to the point where a cloud-to-ground flash struck ground, and the system then triangulated from two or more stations to locate the strike point. Archived data included the time, location, number of strokes, peak signal amplitude of the first stroke (approximately proportional to peak return stroke current), and the polarity of current for each ground flash detected by the system. An examination of amplitude and return stroke rates found little or no systematic evolution of either one relative to evolution of the storm system for this case, so the remainder of this paper focuses upon flash location and polarity.

Previous work indicates that the NSSL network detected approximately 70% of the cloud-to-ground flashes occurring within its region of coverage (Mach et al. 1986). Systematic errors in the azimuths to lightning strikes measured by each station in the network were estimated and removed as discussed by MacGorman and

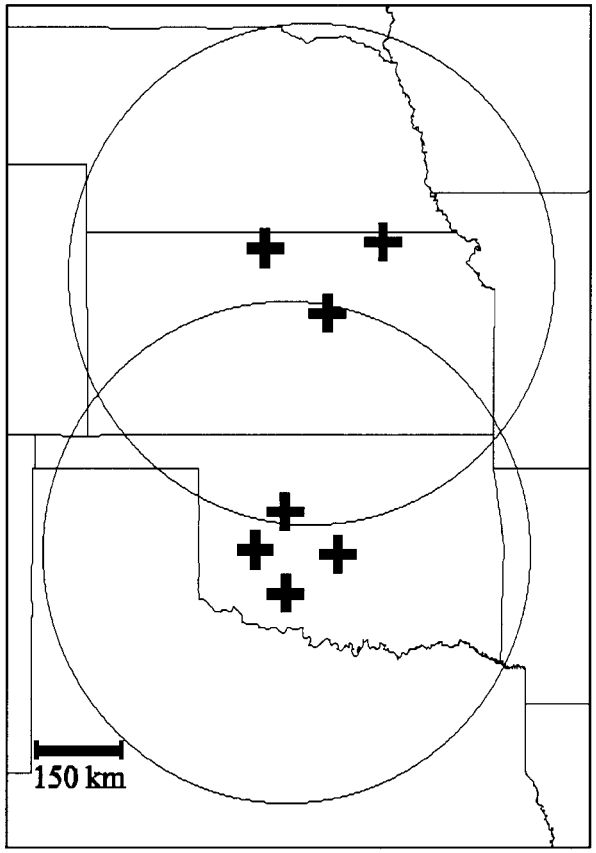

FIG. 2. Locations and coverage of the NSSL lightning location network. Direction finders are indicated by (+). The circles indicate the nominal range of the detection network.

Nielsen (1991). The residual error in azimuths measured by a DF station was typically 1°–2°. Location errors depended upon the location of the flash relative to the network geometry. At the edges of network coverage, errors in ground flash locations typically were 10–20 km. Because the storms in this study were near the center of the network, flash location errors are expected to be no more than 5 km, and most errors are expected to be within roughly 2 km. For a detailed discussion of sources of errors see Krider et al. (1980). More information about the NSSL network and the analysis used to produce archived data is provided by Mach et al. (1986) and by MacGorman and Nielsen (1991).

3. Methodology

To examine spatial relationships between cloud-to-ground lightning, radar data, and hail reports, the locations of lightning strikes to ground and the locations of hail reports were superimposed on contour plots of both base-scan reflectivity (by VIP level) and VIL for each volume scan. The ground flash locations and hail reports plotted for each volume scan were from a 10-min window centered on the time of the volume scan, an interval that corresponds roughly with the 10–12-minute sampling period of the radar data. Mean cell motion for the case was approximately 30 km h^{-1}. This causes errors in alignment of radar data with ground flashes. However, because ground flash data (and hail report locations) were plotted within a window centered upon the radar scan time (5 min either side of the indicated time), the errors in the placement of lightning strikes relative to radar echoes due to storm motion do not exceed 2.5 km, less than one RADAP II grid box, and so can be ignored.

Severe weather reports were obtained from the National Climatic Data Center (1985). Comparing hail reports with lightning and radar data has inherent problems, because hail must be observed by a person to be reported. Often large hail occurs in sparsely populated areas and, therefore, may not be detected. Also, the location and time of a severe weather report sometimes is only approximate, because it is entered after the reported event has occurred. Therefore, a severe weather report well away from storms detected by radar at the reported time may actually be well aligned with an echo from a different volume scan. To compensate for the imprecise times and locations, we adjusted plotted hail reports up to 20 min in time and 5.6 km (3 n mi) in location to improve agreement with radar signatures, as done by Winston and Ruthi (1986).

Aggregate spatial relationships were examined by comparing VIP, VIL, ground flash statistics, and hail coverage. Using the VIL grid, we determined the maximum VIP and VIL values for each RADAP II 5 km × 8 km grid box during any radar volume scan. The cumulative number of ground flashes and maximum ground flash rate were computed for each grid box. A grid box's maximum flash rate was computed by finding the maximum number of ground flashes that occurred in that box during the 10-min window for any RADAP II volume scan during the storm's life span and then dividing that number by 10 to convert it to flashes per minute. These gridded data depicted maxima of VIP, VIL, and flash rate and the cumulative distribution of ground flashes. We then overlaid a plot of all hail reports to compare with these images. Overlays of each field allowed for direct comparison of these storm characteristics.

Besides visual inspection of the spatial distribution of ground flashes, the average density of ground flashes and the probability of observing a ground flash were examined as a function of VIP and VIL for the whole storm system and for various stages of the system's life cycle. Because VIL values varied continually, they were grouped into ranges (Table 2). The average density of ground flashes was computed by counting the number of flashes in grid boxes with a particular value of VIP or a particular range of VIL and then dividing by the total area of grid boxes with that value or range. The flash relative frequency was given by the fraction of

TABLE 2. VIL ranges vs probability of large hail determined by Devore (1983).

VIL range*	Probability**
0	0
5–15	0
20–35	0–20
40–55	20–95
60–80	95–100

* VIL in kg m^{-2}.
** Probability of large hail in %

grid boxes having a particular VIP value or VIL range that also had at least one ground flash.

Histograms of flash density and of flash relative frequency were examined both for the storm system as a whole and for three contiguous 3-h intervals spanning the life of the storm system, to see if relationships varied as the storms matured. The drawback to using shorter time periods was that fewer samples were available for these histograms. However, using shorter periods was useful in showing some broad differences in flash activity between the early and later stages of the storm system.

Time series plots also were produced to examine the overall storm evolution of VIP, VIL, and flash activity. Maximum and average VIP and VIL values were found for all available scan times. Average VIP and VIL values were calculated using only nonzero grid boxes (VIP $\geq$ 1; VIL $\geq$ 5 kg m^{-2}). Positive and negative ground flash rates were determined for 10-min windows centered on radar scan times. When radar data for a particular scan were missing, lightning data and the associated flash products were calculated by using a time window centered about an assumed time for the missing scan (the lightning data had no periods of missing data). In such cases, VIP and VIL and products derived from them were linearly interpolated between values from the first scan before and the first scan after the missing scan.

4. Storm observations

a. Overview of the storm system

The storm system that began in Oklahoma on 26 May 1985 produced a strong mesocyclone and severe weather, including 42 reports of large hail. Base-scan reflectivity for the storm system is plotted in Fig. 3 at selected times throughout the analyzed period to show the evolution of the storm system. The first radar reflectivity echoes were detected at 1630 central standard time (CST), as storms began developing along and ahead of a dryline in western Oklahoma. At 1720 CST, the radar began to detect a new cell forming ahead of the dryline storms. Shortly afterward, cells in both groups began to intensify, with VIL and maximum reflectivity increasing rapidly. Continued development led to two lines of storms, one oriented along the dryline and another 60 km ahead of the dryline thunderstorms.

One storm was particularly interesting because it was the only storm in the system in which a mesocyclone was detected. This storm was first detected at 1750 CST in the line of storms closest to the dryline. It grew from VIP 2 to 5 (30 to 50 dBZ) in 20 min and remained at or above VIP 5 until it became indistinguishable from a subsequent east–west convective line at roughly 2200 CST. During this time, the cell produced seven reports of large hail. The mesocyclone was first indicated by the NSSL Doppler radar at 2031 CST, thereby marking the beginning of the storm's supercell stage, and remained intact until 2100 CST, after which the supercell began to dissipate. Development of new convection along the outflow boundary from the supercell caused the storm system to take on the form of a single east–west line of storms.

Shortly thereafter, a region of stratiform precipitation developed north of the new convective line. Convective intensity indicated by both VIL and reflectivity values declined to a minimum near 0000 CST on 27 May, but reintensified over the following hour. After 0100 CST, radar again indicated a significant weakening and decreased organization of cells along the convective line. No reports of severe weather were noted after 0100 CST.

Time series plots of maximum and average VIP and VIL levels are shown in Figs. 4 and 5. Maximum VIP values rose quickly, with a VIP 6 echo existing somewhere in the domain during most of the storm system's life cycle. Average VIP values provided more information about the overall intensity of precipitation, showing a downward trend late in the life cycle, as the region of stratiform precipitation developed.

The VIL time series plots exhibited much more variability. Maximum VIL increased rapidly shortly before 1800 CST, declined to a minimum at approximately 0000 CST, and increased to a secondary maximum at approximately 0100 CST. Because high VIL values are limited primarily to convective regions, the downward trend in average VIL values (grid boxes in the average were restricted to those with VIL $\geq$ 5 kg m^{-2}) between 2300 and 0000 CST is likely indicative of a decrease in the strength of the convection.

First reports of large hail were recorded at 1810 CST, 100 min after the first echoes were detected (Fig. 6). Maximum VIL values at that time were 65 kg m^{-2}. Hail reports were continual during the next 5 h and were then followed by a period of no reports lasting until 0100 CST. The decline in hail reports corresponded to the decrease in VIL values mentioned previously, and subsequent hail reports coincided with the secondary maximum of VIL values.

b. Overview of lightning ground flash evolution

Relatively few ground flashes occurred during the initial stages of storm development. Positive and negative CG flash rates are shown in Fig. 7 for 10-min time windows centered on radar volume-scan times. As has

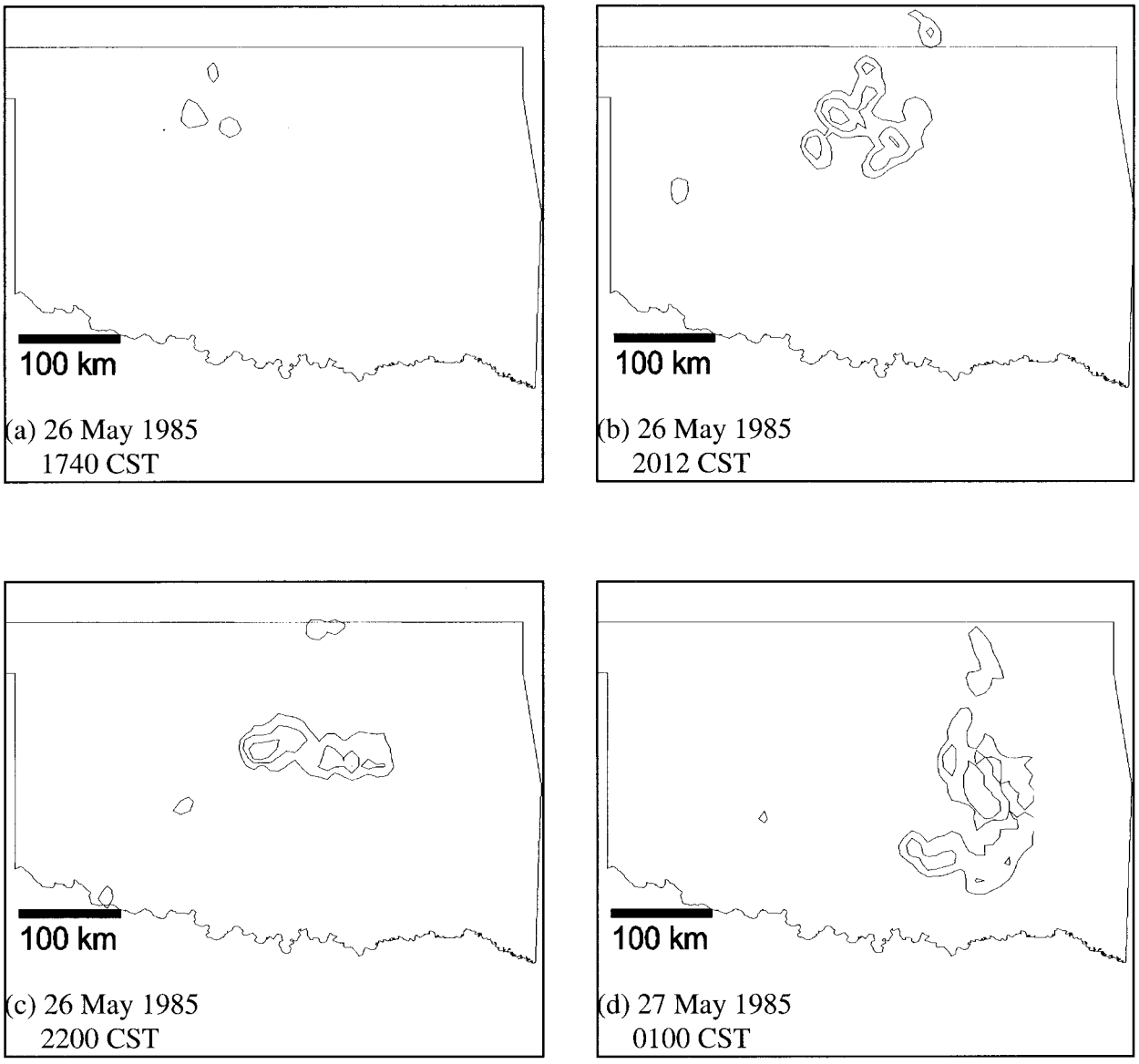

FIG. 3. Radar reflectivity for selected times that depict evolution of the storms on 26–27 May 1985: (a) early stages of storm development featuring individual cells; (b) two lines of cells, one along the dryline and the other 60 km ahead of the dryline storms; (c) single line of cells along an outflow boundary; and (d) single line with trailing stratiform precipitation region. Reflectivity is in VIP level, from 1 to 5 with a contour interval of 2.

often been observed, ground flash rates displayed cycles with periods similar to typical periods of convective cell growth and decay (e.g., MacGorman and Rust 1998). The first flashes were not recorded until 1740 CST, 70 min after the first radar echoes. This was 20 min after VIL values rose to over 5 kg m^{-2} and at approximately the same time that maximum and average VIL began to increase rapidly to 60 and 20 kg m^{-2}, respectively. Cloud-to-ground flash rates remained low until 1910 CST; the maximum flash rate before 1910 CST was 1.2 flashes per minute at 1840 CST.

During the initial stages of lightning activity, from the first flash at 1740 CST until almost 1900 CST, storms in the leading line produced 11 +CG flashes and only 3 −CG flashes (Figs. 8 and 9), while storms along the dryline produced mostly −CG flashes (18 −CG flashes, 3 +CG flashes). After 1900 CST, a mixture of +CG and −CG flashes occurred (Fig. 10), although +CG flash rates tended to be lower and steadier than −CG flash rates. The leading line of storms produced both +CG and −CG flashes more prodigiously than did the dryline storms (Figs. 10 and 11) and accounted for most of the increase in ground flash rates from 1900 CST until the mesocyclone began dissipating at 2100 CST.

Once ground flash rates increased to more than 5 min^{-1} at 1950 CST, they remained above that threshold

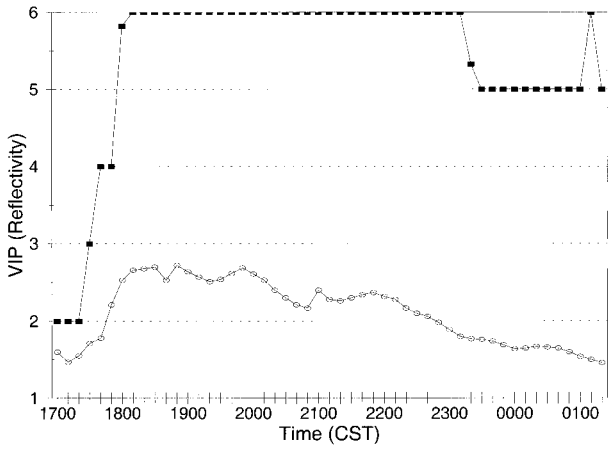

FIG. 4. Time series of maximum (thick lines) and average (thin lines) VIP values over the whole Oklahoma City RADAP II radar range from 1700 CST on 26 May 1985 until 0120 CST on 27 May. Each point in the curve represents a single scan. VIP levels indicate the values of radar reflectivity given in Table 1.

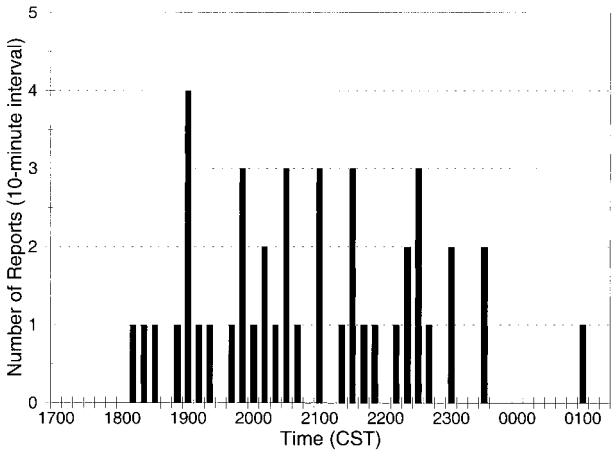

FIG. 6. Number of large hail reports in the study area during each 10-min time window for the duration of the storm system.

until 0200 CST, when the storm system was dissipating. Flash rates peaked at 20 min^{-1} at 2130 CST (Fig. 7) during a large transient pulse in ground flash rates corresponding to the collapse of the cell that contained the mesocyclone (Fig. 12). Thereafter, ground flash rates remained at a lower, but still large, value as the east–west line of storms formed (Fig. 13). When convection in the squall line began decreasing in intensity (Figs. 14 and 15), ground flash rates tended to decline. Shortly after 0000 CST, the convective line reintensified and ground flash rates again increased (Fig. 16), prior to the storm system's final dissipation.

Both of the short lines of storms that preceded formation of the squall line produced reports of large hail; there were 15 reports for the dryline storms from 1800 to 2100 CST and 5 for the leading line of storms during the same period. The high concentration of positive ground flashes with a hail-producing cell in the leading storms (Fig. 9) corresponds well to the findings of a climatological study by Reap and MacGorman (1989), in which high +CG flash densities were likely to be associated with large hail. However, the production of +CG flashes did not appear to be a necessary condition for large hail, since large hail also was reported from dryline storms that produced no ground flashes and later was reported in storms dominated by −CG ground flashes. MacGorman and Burgess (1994) reported a similar observation: When a storm's ground flash activity was dominated by +CG flashes, the storm usually produced large hail, but large hail also occurred in some storms whose ground flash activity was dominated by −CG ground flashes, though in a much smaller fraction of those storms.

The most obvious difference in trends of VIL (Fig. 5) and ground flash rates (Fig. 7) was the lag of approximately 100 min between the onset of precipitation and moderate to large ground flash rates. Once ground

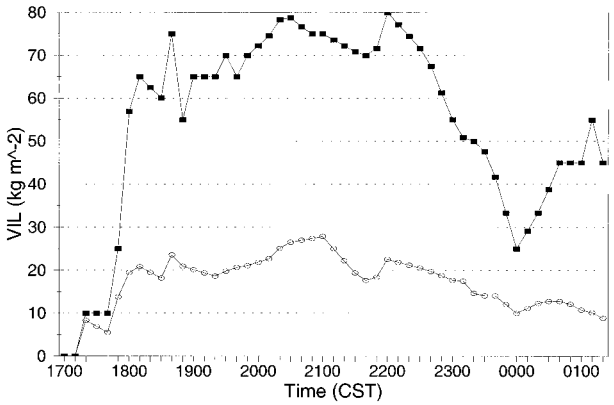

FIG. 5. Time series of maximum (thick lines) and average (thin lines) VIL values over the whole Oklahoma City RADAP II radar range. Each point in the curve represents a single volume scan.

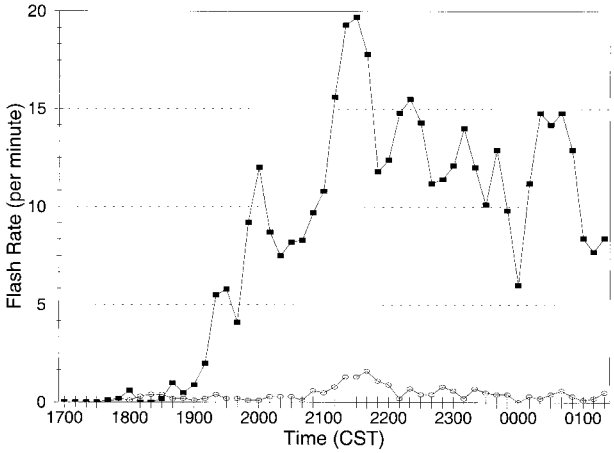

FIG. 7. Time series of ground flash rates (average value in each 10-min interval). Negative ground flashes are indicated by the thick line, and positive by the thin line.

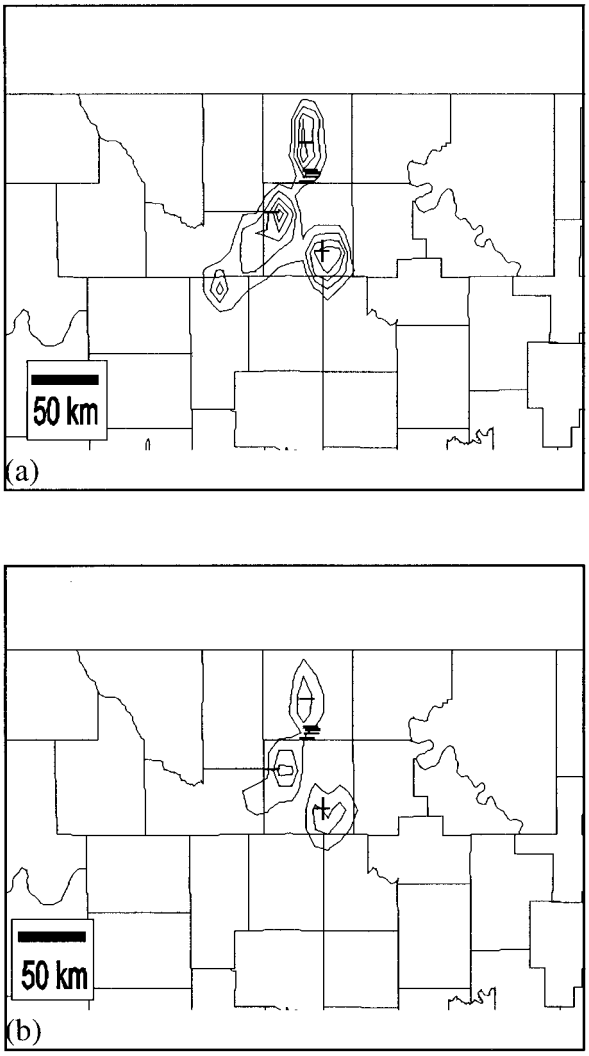

FIG. 8. Ground flashes superimposed on (a) reflectivity and (b) VIL for 1801 CST 26 May 1985. Ground flashes occurred in a 10-min window centered on 1801 CST. Negative ground flashes are indicated by (−), and positive by (+). Reflectivity contours indicate VIP levels, ranging from 1 to 6 in increments of 1. VIL contours range from 5 to 80 kg m^{-2} in increments of 15 kg m^{-2}. During this time period, there were six −CG flashes, one +CG flash, and no hail reports.

flash rates became moderate, trends in both VIL and ground flash rates were qualitatively similar, although there still were obvious differences. Both showed an upward trend until 2000 CST, when VIL levels peaked. VIL values remained near their peak until 2210 CST, when the storm system had just evolved into a single east–west line. Maximum VIL peaked roughly when the mesocyclone formed, while ground flash rates peaked more than an hour later, during the mesocyclone's dissipation, when maximum VIL values still were high.

Both VIL and ground flash rates began to decrease beginning at roughly 2230 CST, when the squall line began decreasing in intensity. However, the decrease in ground flash rates was not as monotonic as that of VIL;

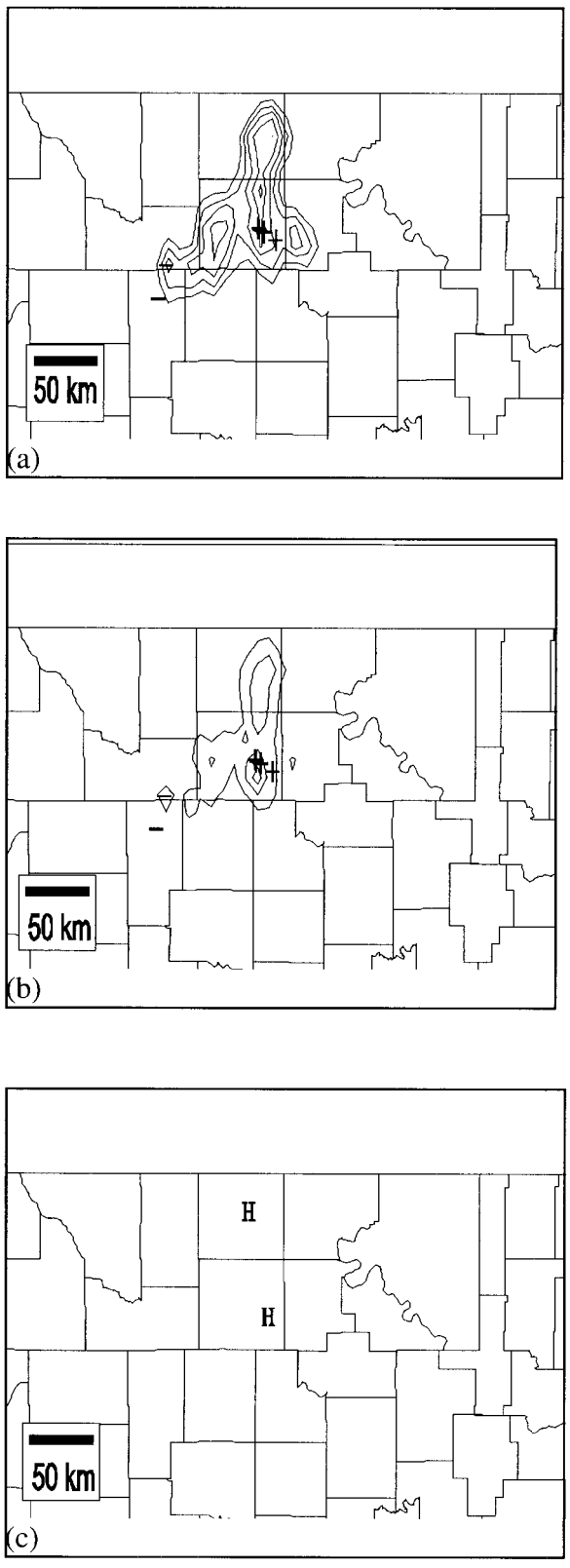

FIG. 9. (a) Reflectivity and ground flashes, (b) VIL and ground flashes, and (c) hail reports for 1830 CST. Symbols and contours are as in Fig. 8. Hail reports within the time window are each indicated by H. There were two −CG flashes, four +CG flashes, and two hail reports.

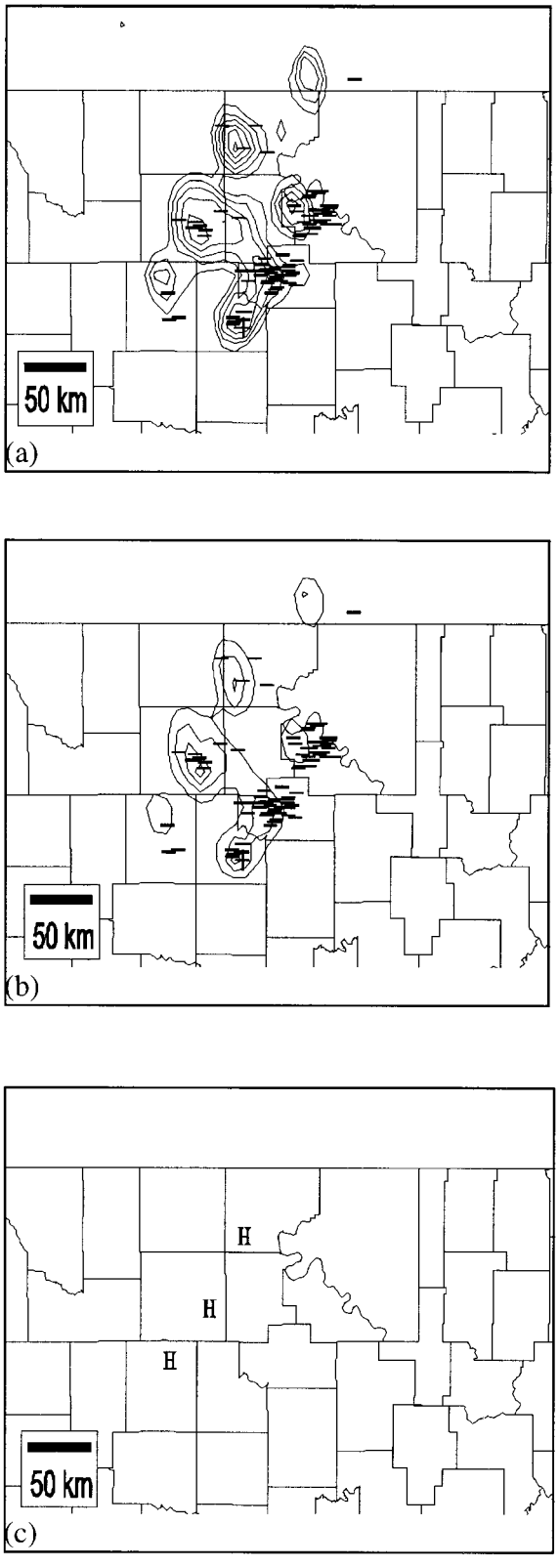

FIG. 10. (a) Reflectivity and ground flashes, (b) VIL and ground flashes, and (c) hail reports for 1950 CST. Symbols and contours are as in Fig. 8. There were 95 −CG flashes, one +CG flash, and three hail reports.

ground flash rates had two sizeable oscillations during the period of decreasing VIL. Both VIL and ground flash rates reached their minimum at roughly 0000 CST, but ground flash rates then increased to a secondary maximum in only 15–20 min, while VIL took 70 min to reach its secondary maximum. In fact, ground flash rates had begun to decrease from their secondary peak approximately 30 min before VIL reached its secondary peak, and so provided an earlier indication of the final dissipation of the system.

c. Analysis of cumulative storm parameters

Summaries of the spatial distribution of storm characteristics are presented in Figs. 17 and 18. Although the passage of time is not indicated in the plots, the effect of a general southeastward motion is apparent in both plots, as is northward growth along the dryline and the slow development of dryline storms. One notable feature is the lag between VIL and lightning ground flash density. Although VIL attained high values in the western part of the region of storm activity, ground flash totals did not increase until the storm complex moved approximately 40 km farther east. This shift was caused by two factors: 1) the tendency for the leading line to produce more ground flashes than the dryline storms and 2) the delayed production of lightning by dryline storms until they moved farther east.

Once ground flash production increased, the distribution of ground flashes was similar to that of maximum VIL, suggesting that most flashes occurred within the more convective regions. The distribution of hail reports also coincided with the VIL maxima (Fig. 17), and later with the ground flash maxima (Fig. 18) after flash rates increased. However, several of the reports of large hail occurred in the early dryline storms, and so fell outside the envelope of significant ground flash activity. High ground flash rates later in the system's lifetime enlarged the envelope toward the east, beyond the area encompassed by hail reports.

We further examined cumulative relationships of ground flash density and relative frequency to both VIL and VIP by tabulating corresponding values for each parameter in every 5 km × 8 km grid box and then plotting the results in histograms. The histogram of ground flash density versus VIP is shown in Fig. 19 (data used in the calculations are presented in Table 3). Ground flash density increased monotonically with increasing VIP level, a result similar to that obtained by Reap and MacGorman (1989), who used a larger grid box (48 km × 48 km, i.e., 2304 km^2 instead of 40 km^2). The similarity of the results from this study, which used grid boxes comparable in size to individual cells, with results from the Reap and MacGorman (1989) study, which used grid boxes that typically encompassed entire storms, suggests that there is a similar tendency for both individual cells and entire storms to have higher ground flash densities as their peak reflectivities increase.

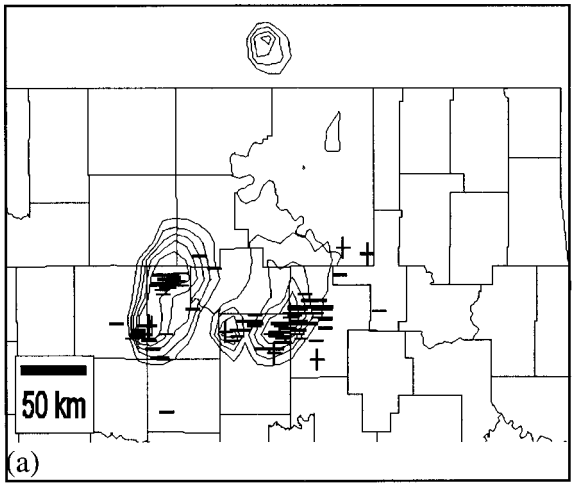

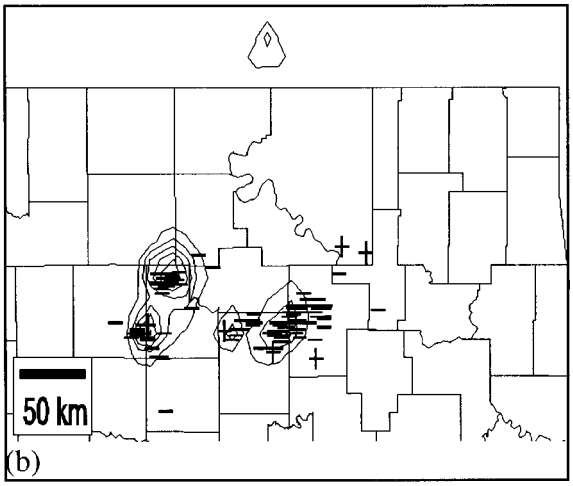

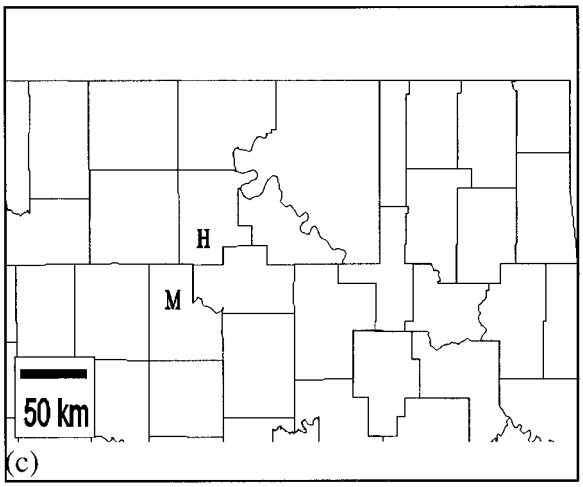

FIG. 11. (a) Reflectivity and ground flashes, (b) VIL and ground flashes, and (c) hail reports for 2100 CST. Symbols and contours are as in Fig. 8. There were 107 −CG flashes, 7 +CG flashes, and one hail report. The mesocyclone is indicated by M.

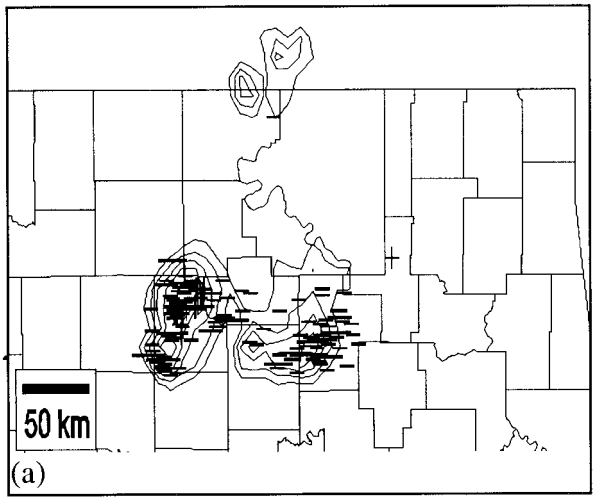

FIG. 12. Ground flashes superimposed on reflectivity for 2114 CST. Symbols and contours are as in Fig. 8. There were 159 −CG flashes, 12 +CG flashes, and no hail reports. VIL data were not available for this time.

Since there was a nearly 3-h lag between the early echoes and the rapid rise in lightning activity, we separated the histogram analysis into three 3-h intervals. The effect of the lack of lightning early in the period is readily apparent in the resulting distributions. Figure 20 shows the flash density during the early stages of storm growth (1700–2000 CST) and during middle stages (2000–2300 CST), when ground flash rates were greatest. The very small number of flashes during early stages is apparent, and the increase in flash density with increasing VIP level is much smaller than for the entire 9-h period. The VIP curve for the period with largest ground flash rates, on the other hand, showed a sharper rise and achieved higher ground flash densities than in the cumulative analysis. The third segment (2300–0200 CST, not shown) differed little from the middle segment; the relationship between ground flash density and VIP varied little once ground flash rates increased.

The histogram of ground flash density versus VIL for the entire storm system is shown in Fig. 21 (data used in the calculations are presented in Table 4). Like VIP, an upward trend in the VIL distribution is apparent, although the shape of the curve differs from the distribution relative to VIP. The concentration of flashes in regions of high VIL values agrees well with qualitative results from the spatial summary plots; maxima in total flash production tended to be coincident with VIL maxima. The changes in the distribution of flash density relative to VIL during the three stages of the storm system were qualitatively very similar to those for VIP, and so are not shown. In particular, the minimum and maximum flash densities observed in the VIL and VIP histograms were similar during corresponding stages of the storm system, as should be expected.

To examine how often grid boxes having particular

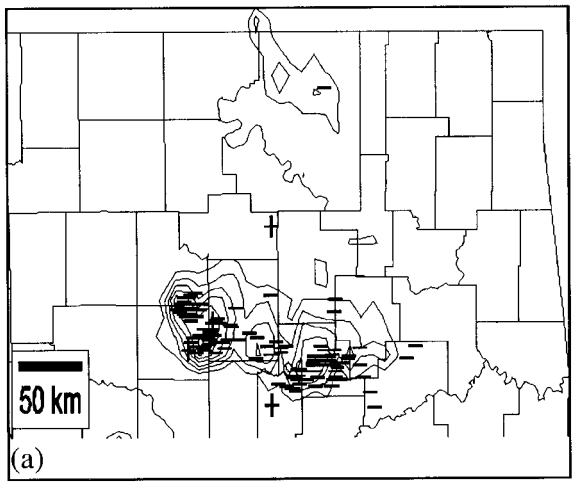

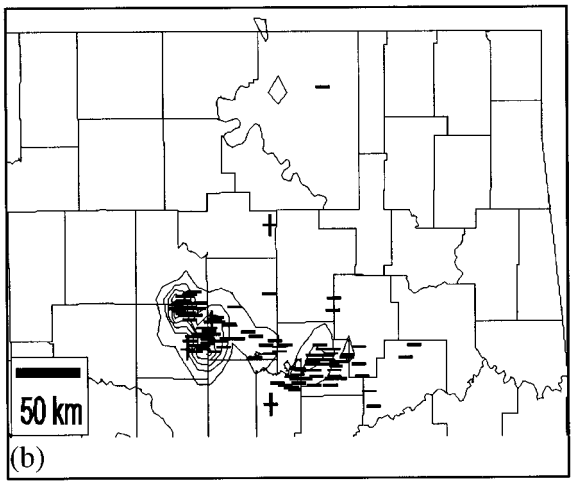

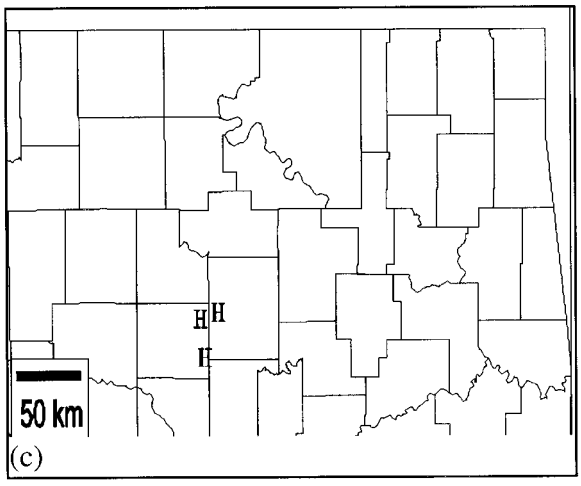

FIG. 13. (a) Reflectivity and ground flashes, (b) VIL and ground flashes, and (c) hail reports for 2236 CST. Symbols and contours are as in Fig. 8. There were 124 −CG flashes, 4 +CG flashes, and three hail reports.

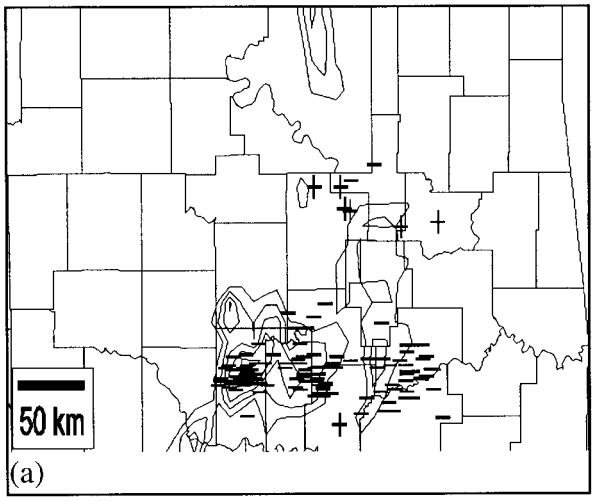

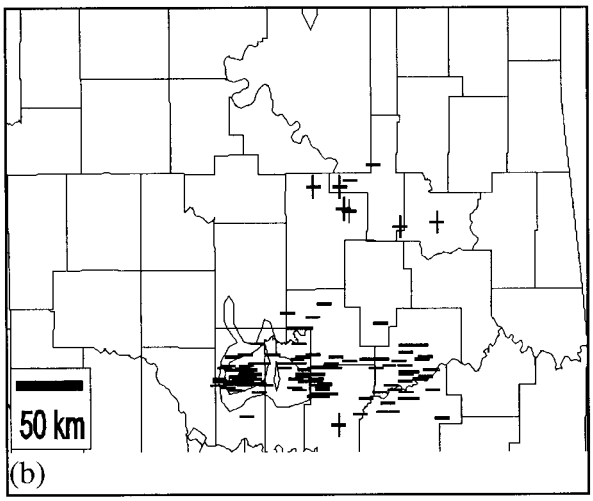

FIG. 14. (a) Reflectivity and ground flashes and (b) VIL and ground flashes for 2324 CST. Symbols and contours are as in Fig. 8. There were 117 −CG flashes, 7 +CG flashes, and no hail reports.

values of VIL or VIP had any ground flash activity during the corresponding 10-min period, we tabulated the relative frequency of one or more ground flashes occurring in the corresponding grid box. The occurrence of ground flashes became more likely with increasing values of both VIP and VIL (Figs. 22 and 23, respectively). In neither histogram, however, did the relative frequency exceed 50%, even at the highest values of VIL and VIP. Although relative frequency increased with increasing values of both VIP and VIL, there were significant differences between them. The relative frequency increased roughly linearly with increasing VIP. However, ground flashes rarely occurred in regions where VIL was less than 5 kg m^{-2}, but became much more common once that threshold was reached. Furthermore, there was only a slight increase in the relative frequency when VIL values increased from 40–55 to 60–80 kg m^{-2}.

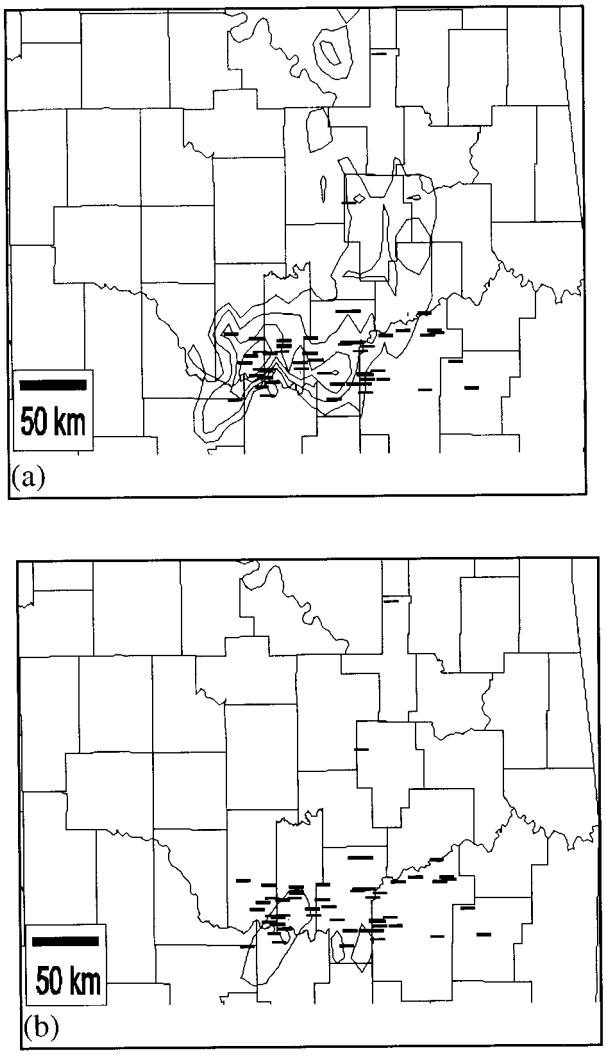

FIG. 15. (a) Reflectivity and ground flashes and (b) VIL and ground flashes for 0000 CST 27 May 1985. Symbols and contours are as in Fig. 8. There were 58 −CG flashes, no +CG flashes, and no hail reports.

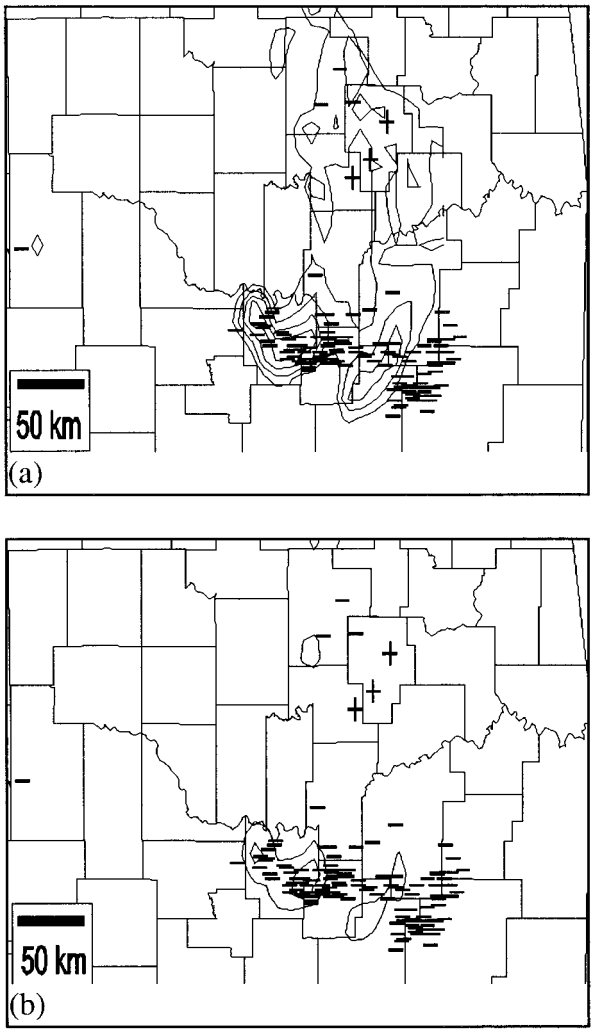

FIG. 16. (a) Reflectivity and ground flashes and (b) VIL and ground flashes for 0050 CST. Symbols and contours are as in Fig. 8. There were 124 −CG flashes, 4 +CG flashes, and no hail reports.

As might be expected from data presented in the previous section, the relative frequencies changed considerably in most bins of VIP and VIL as the storm system evolved from its early to middle stages (Figs. 24 and 25). During the first 3-h period, flashes were recorded in no more than 30% of grid boxes with high VIP or VIL values. During the second and third 3-h periods, relative frequency increased more rapidly with increasing VIP, reaching a maximum value of almost 60%. During these last two 3-h periods the relationship with VIL was significantly different from the relationship with VIP. The relative frequency of ground flashes was nearly 60% for all ranges of VIL greater than 20 kg m^{-2}, suggesting that the production of at least one flash is no more common at extreme VIL values than at moderate values; note, however, that the small sample size in the bin of largest VIL makes conclusions regarding extreme values of VIL less reliable.

Using lightning ground flash data to infer the presence of large VIL, and hence a significant probability of large hail, is problematic. The roughly flat distribution of relative flash frequency with increasing VIL above 20 kg m^{-2} during the second two stages of the storm system suggests that the simple existence of ground flashes cannot be used to make inferences about the probability of large hail. This again is consistent with the earlier findings in the literature that coverage of ground flash activity could not be used in this way. In the present case, the histograms of ground flash density (as opposed to the occurrence of one or more ground flashes) suggest that it might be a useful proxy for VIL and large hail detection, but other studies already show this to be unfeasible. For example, Reap and MacGorman (1989) found that the probability of severe weather, including

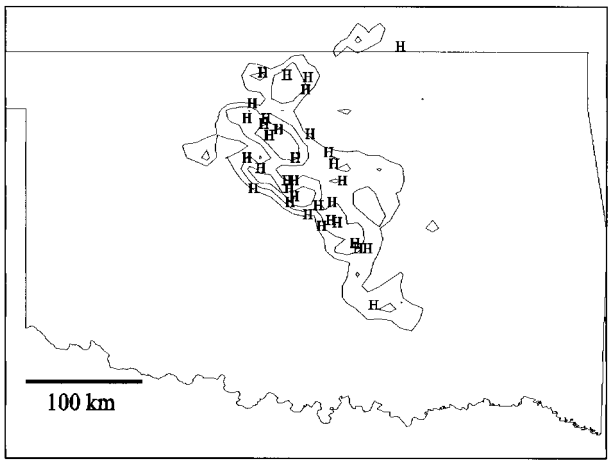

FIG. 17. Maximum VIL values occurring in each 5 km × 8 km grid box during the storm's life span (1630 CST 26 May–0120 CST 27 May 1985) overlaid with hail reports (H). Contours of VIL range from 20 to 80 kg m^{-2}, with a contour interval of 20 kg m^{-2}.

large hail, changes only slightly with increasing −CG flash density and, in fact, decreases at the largest values of −CG flash density. The only ground flash parameter that published studies suggest may be related to the occurrence of large hail is the density of +CG flashes (e.g., Reap and MacGorman 1989; MacGorman and Burgess 1994). Positive cloud-to-ground flashes will be discussed further in the next section.

5. Discussion

The study to this point has focused upon storm evolution, trends in the variables being studied, and the cumulative relationships between cloud-to-ground lightning and digitized radar data. Each of these parts is examined in more detail in this section with the intent of relating the observations described above to other observations and hypotheses presented in the literature.

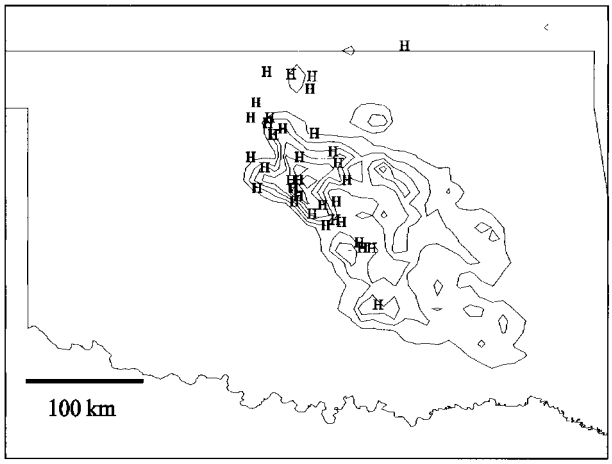

FIG. 18. Number of ground flashes in each 5 km × 8 km grid box overlaid with hail reports (H) from 1630 CST 26 May to 0120 CST 27 May 1985. Contoured values range from 2 to 22 flashes, with a contour interval of 4.

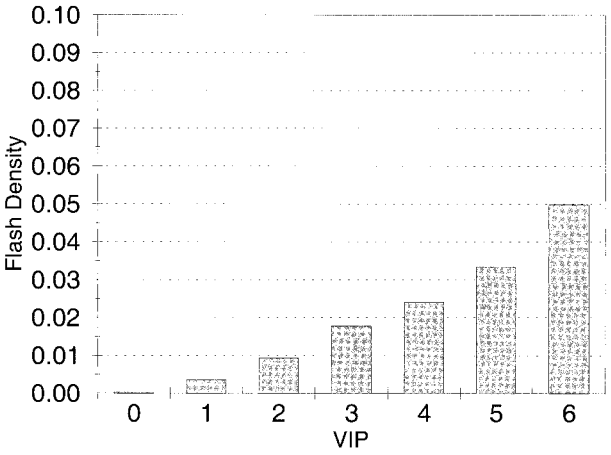

FIG. 19. Ground flash density vs VIP level. Each 5 km × 8 km grid box of each 10-min period was included in the ensemble for computing ground flash density, and ground flash count and VIP level were tabulated for each. The total number of ground flashes in all grid boxes having a given value of VIP level was divided by the total area of those grid boxes (number of grid boxes times 40 km^2) to get ground flash density. The data used in the calculations are in Table 3.

a. *Ground flashes relative to radar reflectivity parameters*

The primary focus of this research was upon relationships between digitized radar reflectivity parameters and ground flash data. There were considerable similarities in the trends of these properties. In particular, the spatial patterns of ground flash density were similar to those of reflectivity and VIL, with the largest flash densities tending to occur in and near regions of large reflectivity and VIL. Furthermore, the temporal trends in ground flash rates were similar to those of average VIL in that both parameters peaked and then decreased to a minimum at approximately the same time.

The most obvious exceptions to similarities in trends of ground flashes and reflectivity parameters occurred early in the life of the storm system, when storms were

TABLE 3. Ground flash density and relative frequency by VIP level, for storm's lifetime.

VIP	No. of flashes	No. of grid boxes	No. of boxes with flashes	Flash density	Flash relative frequency*
0	691	146 287	448	0.0002	0.3
1	390	3969	241	0.0035	6.0
2	611	2359	357	0.0093	15.1
3	400	809	189	0.0178	23.4
4	500	746	212	0.0241	28.4
5	448	483	181	0.0334	37.5
6	191	138	61	0.0498	44.2

* In %.

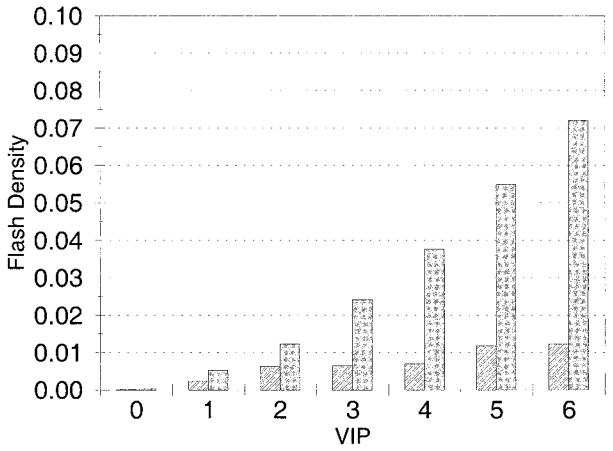

FIG. 20. Ground flash density vs VIP level in the early stages of the storm system (1700–2000 CST; hatched bars) and in the middle stages (2000–2300 CST; solid bars) when ground flash rates were highest.

forming along and ahead of the dryline. There were no ground flashes until maximum reflectivity increased to VIP level 4 (46 dBZ) and maximum VIL began to increase above 10 kg m^{-2}. Furthermore, ground flash rates remained low for more than an hour after the first flash, remaining $\leq$1.2 min^{-1} until there was rapid growth in the number of cells in the leading line of storms.

Of course, the lack of ground flash activity cannot be assumed to mean that there was no lightning activity. Usually the initial flashes in storms are cloud flashes [i.e., flashes not striking ground; e.g., Krehbiel (1986)], and sometimes there are few, if any, ground flashes in severe storms that have frequent cloud flashes (e.g., MacGorman et al. 1989). In fact, some trained observers who chase thunderstorms have suggested that vigorous Great Plains thunderstorms having very large overall flash rates, but little ground flash activity, are likely to

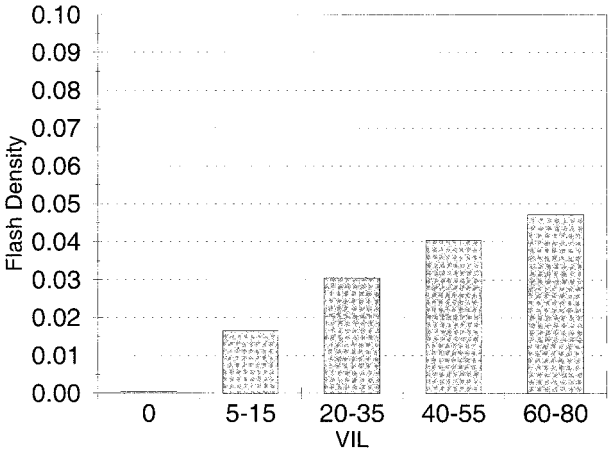

FIG. 21. Ground flash density vs VIL. The calculation of ground flash density for VIL intervals is analogous to that for VIP level, described in the caption for Fig. 19, with VIL interval replacing VIP level. The data used in the calculations are in Table 4.

TABLE 4. Ground flash density and relative frequency by VIL range, for storm's lifetime. VIL values were grouped into ranges according to probability of large hail from Devore (1983).

VIL	No. of flashes	No. of grid boxes	No. of boxes with flashes	Flash density	Flash relative frequency*
0.00	1263	132 831	850	0.0003	0.6
5–15	594	1290	319	0.0166	24.7
20–35	674	559	187	0.0305	33.4
40–55	201	179	76	0.0404	42.4
60–80	114	87	40	0.0472	46.0

* In %.

be severe and frequently produce large hail. Thus, the observation of large hail in storms having no ground flash activity, as on 26 May, is not without precedence. However, no data on cloud flashes are available for this case, so we cannot determine whether the storms on 26 May were electrically active during early stages of their production of large hail, though observations of other storms suggest they likely were.

The overall relationship between cloud-to-ground lightning and VIL is consistent with that observed by Watson et al. (1995), who examined relationships between VIL and ground flashes using a similar size grid box for an Oklahoma squall line. Though the intervals of VIL in their bar plots are different from those used in this study and so cannot be compared in detail, the relationship they found between ground flash occurrence and VIL is grossly similar to that shown in Fig. 23. The average density of ground flashes also tends to increase with increasing VIL, but Watson et al. found that most flashes occurred in regions of low VIL, with the total number of flashes decreasing in grid boxes of

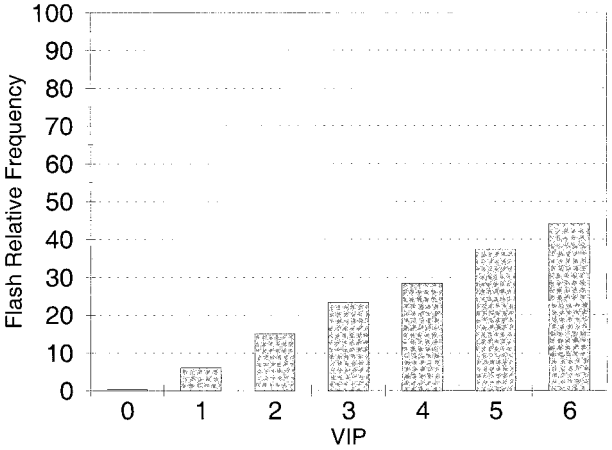

FIG. 22. Probability (in %) of observing a ground flash in a grid box in 10 min as a function of VIP level. Each grid box of each 10-min period is included in the ensemble for computing flash relative frequency. The flash relative frequency was given by the fraction of grid boxes having a particular VIP value that also had at least one ground flash. The data used in the calculations are in Table 3.

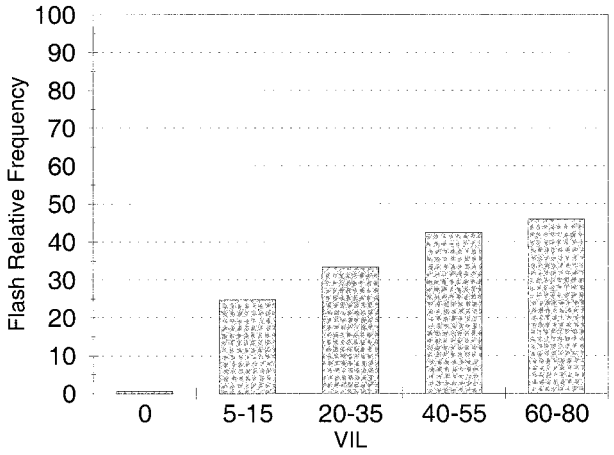

FIG. 23. Probability (in %) of observing a ground flash in a grid box in 10 min as a function of VIL (in the intervals shown). Flash relative frequency for VIL is analogous to that for VIP, described in the caption for Fig. 22, with VIL interval replacing VIP level. The data used in the calculations are in Table 4.

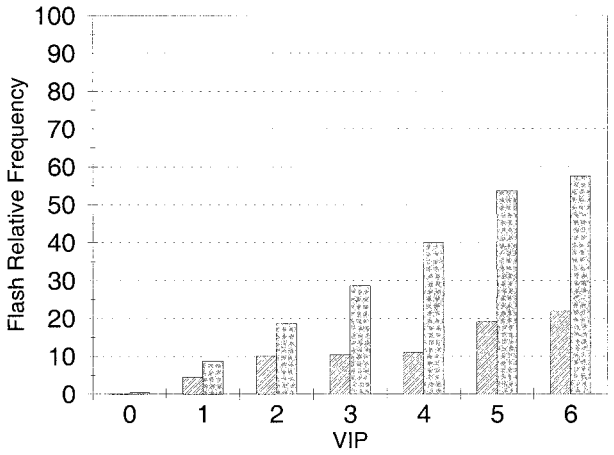

FIG. 24. Probability (in %) of observing a ground flash in a grid box as a function of VIP level for the early stages of the storm system (1700–2000 CST; hatched bars) and for the middle stages (2000–2300 CST; solid bars). Flash relative frequency is defined in the caption for Fig. 22.

larger VIL. Table 4 shows a similar finding for this study, with 44% of flashes occurring in regions where VIL was less than 5 kg m^{-2}. Thus, absolute numbers of flashes are not a good indicator of regions of high VIL. Average flash density and relative frequency are normalized to compensate for the different total areas of grid boxes having different values of VIL; both parameters increase with increasing VIL, as shown in Figs. 21 and 23.

b. Ground flashes relative to large hail reports

Another goal of this study was to examine whether there was any signature in the lightning strike data that indicated the occurrence of large hail. As on the four storm days studied by MacGorman and Burgess (1994), large hail occurred in storms during many periods when the majority of ground flashes comprised +CG flashes, although we do not yet understand why. Furthermore, the sparsity of ground strikes in the strong storm having a mesocyclone may eventually be construed as a lightning signature frequently accompanied by large hail, although more research is needed to establish whether these observations are correlated often enough to have physical meaning.

Both possible signatures provide at best a one-way test: The lightning signature appeared to indicate the presence of large hail, but the absence of the signature did not mean large hail was absent. In fact, large hail reports sometimes clustered in and near regions having an average flash density of at least 5 km^{-2}, but having few if any +CG flashes. Furthermore, during periods when negative flashes dominated ground flash activity, +CG flashes appeared to have little relationship with large hail. In fact, the frequency of large hail reports decreased when +CG flash rates had their largest increase during the collapse of a mesocyclone, when −CG flashes dominated ground flash activity.

Changnon (1992) has also examined relationships between ground flashes and hail for 48 hail streaks. No mesocyclone and no +CG flashes were observed in the storms he studied. Cloud-to-ground lightning was always associated with streaks of hail damage (unlike the early stages of the dryline storms reported here), but not all storms with frequent cloud-to-ground lightning produced hail. Typically, the ground flashes associated with a hail streak began 9 min before hail was observed at the ground and continued until shortly after hail ended. Clusters of lightning strikes to ground tended to be adjacent to hail reports (similar to the pattern shown in

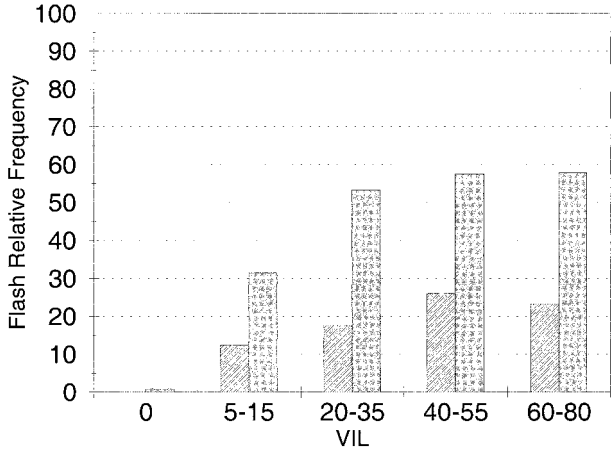

FIG. 25. Probability (in %) of observing a ground flash in a grid box as a function of VIL for the early stages of the storm system (1700–2000 CST; hatched bars) and for the middle stages (2000–2300 CST; solid bars). Flash relative frequency is defined in the caption for Fig. 23.

Figs. 10 and 11), with few strikes inside most regions having hail damage.

In a study concentrating on +CG flashes, Carey and Rutledge (1998) found that large hail began to fall as a storm in Colorado began producing +CG flashes, but that +CG flashes continued to occur after large hail had finished falling. Thus, large hail was associated with only the earlier part of the period when +CG flashes were produced. Hail reports were near, but not coincident with, the location of ground strikes. Too few cases have been analyzed to determine if there is a reasonably consistent relationship between +CG flashes and hail, much less to find if such a relationship differs from one climatological region to another.

Because of VIL's usefulness in helping to detect large hail in Great Plains thunderstorms and because of the good correlation between VIL and large hail reports in this case, one might wonder whether there is any need to find if there is a relationship between +CG occurrence and large hail that is consistent enough to be useful, at least regionally. However, VIL is not a perfect indicator of large hail, even in storms on the Great Plains. Clusters of cloud-to-ground lightning or the presence of +CG flashes may be useful supplements to VIL, if large hail occurs in a readily identifiable set of storms in which these signatures appear.

c. Ground flash polarity during the dryline storms

This is the first case in which ground flash data that include flash polarity have been studied for two lines of storms that formed near a dryline, so the observed distribution of ground flashes by polarity during the dryline storms is particularly intriguing. Only four other studies (Bluestein and MacGorman 1998; MacGorman and Burgess 1994; Curran and Rust 1992; Branick and Doswell 1992) have examined the polarity of ground flashes either in storms that formed near a dryline or in low-precipitation supercell storms, which tend to be more prevalent near drylines.

Curran and Rust (1992) found that the dominant ground flash polarity was positive in a supercell storm that initially had low-precipitation characteristics and then changed to negative as the storm developed classic supercell characteristics. Branick and Doswell (1992) examined ground flash polarity on a day in which widespread severe storms occurred in Oklahoma, Kansas, and Nebraska. They found that ground flash activity in supercell storms having low-precipitation supercell characteristics was dominated by positive ground flashes. Farther southeast, where storm characteristics tended more toward the heavy-precipitation part of the supercell spectrum, ground flash activity was dominated by negative ground flashes.

MacGorman and Burgess (1994) studied several storms that began near a dryline and became supercell storms as they moved eastward. Storms that grew quickly into supercell storms were dominated by positive ground flashes from their first ground flash until the storms underwent a transformation hours later. In other cases, a storm began as part of a group of weak storms and then became a supercell as it grew in height and VIL and began to dominate other storms in the group. In this second type of storm, ground flash activity was dominated by negative flashes when the storm was part of the group, but became dominated by positive flashes when the storm intensified and other storms in the group disappeared. There sometimes was a subsequent transition of the dominant polarity back to negative ground flashes, often as the storm evolved from a low precipitation to a classic supercell storm or from a classic supercell to a high-precipitation supercell storm.

A different pattern was found by Bluestein and MacGorman (1998), who examined four supercell storms that formed near a dryline one day in the Texas panhandle. Only one of the four storms was a low-precipitation supercell, and the dominant ground flash polarity was negative throughout this storm's lifetime. In the last two of the supercell storms, positive ground flashes composed the majority of ground flashes for roughly an hour at the beginning of each storm. In only one of these was the positive ground flash rate ever greater than 1.5 min^{-1}. No obvious difference in storm reflectivity structure appeared to be consistently associated with the different dominant ground flash polarities, but the only radar data available to Bluestein and MacGorman (1998) were photographs of a WSR-57 radar display, so differences could well have been undetected.

On 26 May, the majority of the infrequent ground flashes in the line of storms closest to the dryline were negative ground flashes, while the majority of the more frequent ground flashes in the line that formed 60 km ahead of the initial line were positive ground flashes. This pattern appears reversed from what was observed by Curran and Rust (1992) and Branick and Doswell (1992). In fact, the storms on 26 May in which positive ground flashes initially dominated ground flash activity do not appear to fit any of the patterns observed in either of these two studies or in MacGorman and Burgess (1994). The behavior on 26 May is most similar to that on the day documented by Bluestein and MacGorman (1998) in that the ground flash activity of low-precipitation storms was dominated by negative ground flashes on both days. For neither day is it clear how present hypotheses for the production of positive ground flashes [see discussion by MacGorman and Burgess (1994) and Carey and Rutledge (1998)] explain why some storms on that day produced positive ground flashes and some did not.

d. Ground flashes in the storm having a mesocyclone

Because there have been several previous studies of ground flashes in supercell storms and in mesoscale convective systems, we will briefly describe these aspects

of the present case to put them into the context of earlier studies. However, because cloud flash data are unavailable for the present case, cloud flash rates, which often have been observed to be large when mesocyclones are strong (e.g., MacGorman et al. 1989; MacGorman 1993), cannot be analyzed.

As mentioned previously, the only mesocyclone observed on 26 May occurred in the line of storms nearest the dryline. This line segment initially produced little cloud-to-ground lightning from the time it was first detected by radar at 1700 CST until 1900 CST, though it grew rapidly and had four reports of large hail during this period. Later, during the period when the NSSL Doppler radar indicated the presence of a mesocyclone (2031–2100 CST), this line segment was characterized by moderate ground flash rates and two more reports of large hail. (Figure 11 shows radar reflectivity and VIL just before dissipation of the mesocyclone.) As the mesocyclone dissipated, the ground flash rate of this storm increased from 2 to 5 min^{-1}, accompanied by an increase in the positive ground flash rate from 0 to approximately 1 min^{-1} (Fig. 12). Flash rates remained relatively high for the next hour, as this storm dissipated and new storm development began along the outflow boundary.

Although ground flash rates were larger during the mesocyclone in this storm than during the tornadic stage of the Binger storm studied by MacGorman et al. (1989), they were comparable to rates later in the Binger mesocyclone, when that storm produced no more tornadoes. Furthermore, −CG flash rates in both the Binger storm and the present case increased rapidly as the mesocyclone dissipated. As discussed in the introduction, a similar relationship with mesocyclone dissipation has been noted in a number of tornadic storms, but not in all tornadic storms (see the review by MacGorman 1993). MacGorman and Nielsen (1991) suggested that the storm's charge distribution is affected by a pronounced reflectivity deficit associated with a weak echo region that extends over a large vertical depth. The precipitation deficit in the weak echo region would cause a corresponding deficit in the charge normally carried by precipitation and this can restrict production of ground flashes. When the weak echo region begins filling with precipitation as the mesocyclone dissipates, ground flash rates increase.

As the mesocyclone dissipated on 26 May, +CG flash rates near the mesocyclone also increased considerably. The Binger study and all earlier studies of supercell storms lacked data on +CG flashes, so no direct comparison can be made with those cases. A tendency in some supercell storms for +CG flashes to occur near the mesocyclone sometime during its lifetime has been documented by several investigators, as discussed in section 5c, and has been reported anecdotally for tornadic storms by operational meteorologists. However, many of these other storms produced tornadoes, and +CG flashes usually occurred before or during the tornadoes, instead of increasing during dissipation of the mesocyclone as in the present case. The behavior of lightning polarity for the mesocyclone on 26 May is somewhat like that often observed in small summer thunderstorms by Fuquay (1982), who reported that the last several ground flashes produced by a storm often were positive ground flashes, though almost all ground flashes were negative earlier in the storm.

e. Ground flashes in the mesoscale convective system

As described previously, an east–west squall line had formed along the outflow boundary of the dissipating mesocyclone by approximately 2200 CST and dominated convection in the storm system thereafter. Beginning at 2200 CST, a stratiform precipitation region grew north of the east–west line. Figures 13–16 show the growth in the area of weak reflectivities (much of the area had reflectivity of only VIP 1) north of the line. The distribution of ground flashes in the stratiform precipitation and convective line was similar in many respects to that of other mesoscale convective systems on the Great Plains, studied, for example, by Rutledge and MacGorman (1988), Rutledge et al. (1990), Hunter et al. (1992), Stolzenburg et al. (1994, 1998), and MacGorman and Morgenstern (1998). As in the squall lines studied by these investigators, most ground flashes in the convective line were −CG flashes. Ground flashes became increasingly common in the stratiform region as it grew, with six out of eight flashes in that region being +CG flashes in the analysis for 2324 CST (Fig. 14).

By 0000 CST (Fig. 15) weakening in the convective line was apparent, although the horizontal extent of the stratiform precipitation region continued to grow. Ground flash activity in both the convective and stratiform regions also declined near 0000 CST, to a flash rate less than half that of the previous half hour. Renewed growth in convective activity occurred after 0000 CST along the leading convective line, and ground flash rates in both the convective line and stratiform region also increased (Fig. 16). During reintensification, the percentage of ground flashes in the stratiform region that were −CG flashes was larger than previously. The two ground flashes more than 50 km north of the convective line at 0000 CST were −CG flashes (Fig. 15), and three of seven were −CG flashes at 0050 CST (Fig. 16).

The decrease and subsequent increase in convection and lightning activity during the mesoscale convective system is of particular interest. As noted above, a similar decrease and increase was observed in ground flash rates, VIL, and average reflectivity. However, the most interesting lightning behavior is not so much that the storm system began dissipating and then reintensified, as that ground flashes throughout essentially all parts of the mesoscale convective system showed a similar trend. In particular, the decrease and subsequent increase in

ground flash rates were observed simultaneously in both the convective line and in the stratiform precipitation region, behavior that appears at odds with the continued growth in the area of the stratiform region throughout this period.

It appears to us that this simultaneity may have implications concerning the mechanism by which stratiform precipitation regions become electrified enough to support lightning. There has been considerable controversy over the relative amounts of charge supplied to the stratiform region by charge advection from the convective line and by local charge generation in the stratiform region. The crux of these arguments has concerned the distance over which charge can be advected while maintaining significant charge density. In a recent evaluation of the two mechanisms, Stolzenburg et al. (1994) concluded that both mechanisms could contribute comparable charge densities out to distances that, in most cases, encompass the ground strikes in the stratiform region.

In the present case, the simultaneous and similar trends for ground flash rates in two regions having very different lightning, microphysical, and kinematic characteristics and separated by up to 125 km suggest that a single event or chain of events affected the ground flash activity in both regions. We suggest two possibilities.

1) Large-scale forcing, such as from a short wave, reintensified updrafts in the convective and stratiform regions simultaneously, leading to a corresponding increase in charging and a subsequent increase in ground flash rates in both regions. On 26 May, the base-scan reflectivity in much of the stratiform region increased from VIP level 1 to level 2 between 0000 and 0100 CST, and VIL also increased near several of the lightning strikes in the stratiform region during the same period. These observations appear consistent with an increase in the weak updrafts of the stratiform region. However, not enough data are available to estimate whether an effect on charging in the stratiform region would be expected.
2) Alternatively, the reintensification of electrification occurred primarily in the convective line, but most flashes having ground strikes in the stratiform region were initiated near the convective region, so that ground strike rates in both regions had similar trends. Many, if not most, ground strikes in the stratiform region occur as part of long horizontal flashes spanning at least a few tens of kilometers (e.g., Schuur et al. 1991, pp. 271–272; MacGorman and Rust 1998, p. 280). In the only squall line documented in the literature in which lightning channels inside the cloud have been mapped (Mazur and Rust 1983), many of the long horizontal flashes in the stratiform region began in or near the convective line. However, such data were not collected during PRE-STORM, so we cannot determine whether this was true for ground flashes in the stratiform region on 26–27 May.

6. Conclusions

This case is notable in that it had several types of storms in the course of its life cycle, including a short line of dryline storms, a supercell storm with a mesocyclone, and a mesoscale convective system. While many studies focus upon individual types of storms, this study provides an examination of the evolution of lightning through these various storm stages. In doing so, it corroborates some previous research, but also raises new questions.

The preceding analysis and discussion highlights two features of this case which have not been documented previously in the literature. One of the characteristics observed for the first time is the disparity in the lightning ground flash activity of the initial two lines of storms. Instead of a single line of storms along the dryline, this case had two lines of storms, separated by 60 km. There have been few studies of lightning in dryline storms and none in which there were two parallel lines, as in this case. The pattern of lightning polarity in this case appears contrary to what has been reported in most other cases involving dryline storms thus far, in that the storms closest to the dryline produced more negative ground flashes than positive ground flashes, while the leading line produced more positive ground flashes.

A second observation that has not been reported previously is the roughly simultaneous decrease and subsequent increase in ground flash rates in the convective and stratiform regions that was noted during the MCS stage. Although charge advection from the convective region into the stratiform region may play a role in production of flashes in the stratiform region, advection requires time, so other factors are necessary to explain the simultaneity of trends in ground flash rates of the two regions. Two hypotheses were suggested. 1) Updrafts and the resulting local charge generation were enhanced simultaneously in both regions by some large-scale phenomenon, such as a short wave, or 2) the ground flashes in the stratiform region were long horizontal flashes originating near the convective line and so experienced a trend in flash rates similar to that of ground flashes in the convective region. Because of the lack of data on mesoscale and convective updrafts and on the in-cloud structure of flashes, neither of these hypotheses can be verified with the available dataset. However, the unusual and previously undocumented aspects of this case provide additional foci for further research.

Acknowledgments. This research was supported by NOAA Grant NA85RAH05046. The authors wish to thank Ken Crawford for his guidance and suggestions. We would also like to thank Larry Ruthi and Kurt Nielsen for their help in acquiring the data used in this study

and for providing insight into operational aspects of the study. We thank Ron Holle and Conrad Ziegler for helpful comments on an earlier draft of this manuscript.

REFERENCES

Bluestein, H. B., and D. R. MacGorman, 1998: Evolution of cloud-to-ground lightning characteristics and storm structure in the Spearman, Texas, tornadic supercells of 31 May 1990. *Mon. Wea. Rev.,* **126,** 1451–1467.

Branick, M. L., and C. A. Doswell III, 1992: An observation of the relationship between supercell structure and lightning ground strike polarity. *Wea. Forecasting,* **7,** 143–149.

Carey, L. D., and S. A. Rutledge, 1998: Electrical and multiparameter radar observations of a severe hailstorm. *J. Geophys. Res.,* **103,** 13 979–14 000.

Changnon, S. A., 1992: Temporal and spatial relations between hail and lightning. *J. Appl. Meteor.,* **31,** 587–604.

Cummins, K. L., M. J. Murphy, E. A. Bardo, W. L. Hiscox, R. B. Pyle, and A. E. Pifer, 1998: A combined TOA/MDF technology upgrade of the U.S. National Lightning Detection Network. *J. Geophys. Res.,* **103,** 9035–9044.

Curran, E. B., and W. D. Rust, 1992: Positive ground flashes produced by low-precipitation thunderstorms in Oklahoma on 26 April 1984. *Mon. Wea. Rev.,* **120,** 544–553.

Devore, D. R., 1983: The operational use of digital radar data. Preprints, *13th Conf. on Severe Local Storms,* Tulsa, OK, Amer. Meteor. Soc., 21–24.

Elvander, R. C., 1980: Further studies on the relationships between parameters observed with objectively defined echoes and reported severe weather events. Preprints, *19th Conf. on Radar Meteorology,* Miami Beach, FL, Amer. Meteor. Soc., 80–86.

Fuquay, D. M., 1982: Positive cloud-to-ground lightning in summer thunderstorms. *J. Geophys. Res.,* **87,** 7131–7140.

Greene, D. R., and R. A. Clark, 1972: Vertically integrated liquid water—A new analysis tool. *Mon. Wea. Rev.,* **100,** 548–552.

Hunter, S. M., T. J. Schuur, T. C. Marshall, and W. D. Rust, 1992: Electric and kinematic structure of the Oklahoma convective system of 7 June 1989. *Mon. Wea. Rev.,* **120,** 2226–2239.

Jackson, M. J., and K. C. Crawford, 1988: The use of surface and RADAP-II data to derive short-term hail prediction equations. Preprints, *15th Conf. on Severe Local Storms,* Baltimore, MD, Amer. Meteor. Soc., 213–216.

Krehbiel, P. R., 1986: The electrical structure of thunderstorms. *The Earth's Electrical Environment,* National Academy Press, 90–113.

Krider, E. P., R. C. Noggle, A. F. Pifer, and D. L. Vance, 1980: Lightning direction-finding systems for forest fire detection. *Bull. Amer. Meteor. Soc.,* **61,** 980–986.

MacGorman, D. R., 1993: Lightning in tornadic storms: A review. *The Tornado: Its Structure, Dynamics, Prediction, and Hazards, Geophys. Monogr.,* No. 79, Amer. Geophys. Union, 173–182.

——, and K. E. Nielsen, 1991: Cloud-to-ground lightning in a tornadic storm on 8 May 1986. *Mon. Wea. Rev.,* **119,** 1557–1574.

——, and D. W. Burgess, 1994: Positive cloud-to-ground lightning in tornadic storms and hailstorms. *Mon. Wea. Rev.,* **122,** 1671–1697.

——, and C. D. Morgenstern, 1998: Some characteristics of cloud-to-ground lightning in mesoscale convective systems. *J. Geophys. Res.,* **103,** 14 011–14 023.

——, and W. D. Rust, 1998: *The Electrical Nature of Storms.* Oxford University Press, 422 pp.

——, D. W. Burgess, V. Mazur, W. D. Rust, W. L. Taylor, and B. C. Johnson, 1989: Lightning rates relative to tornadic storm evolution on 22 May 1981. *J. Atmos. Sci.,* **46,** 221–250.

Mach, D. M., D. R. MacGorman, and W. D. Rust, 1986: Site errors and detection efficiency in a magnetic direction-finder network for locating strikes to ground. *J. Atmos. Oceanic Technol.,* **3,** 67–74.

Mazur, V., and W. D. Rust, 1983: Lightning propagation and flash density in squall lines as determined with radar. *J. Geophys. Res.,* **88,** 1495–1502.

McGovern, W. F., R. E. Saffle, and K. C. Crawford, 1984: Verification results from 1982–1984 operational radar reflectivity experiment. Preprints, *22d Conf. on Radar Meteorology,* Zurich, Switzerland, Amer. Meteor. Soc., 188–191.

McGrew, R. G., 1972: Project DRADEX (Digitized Radar Experiments). Preprints, *15th Conf. on Radar Meteorology,* Champaign–Urbana, IL, Amer. Meteor. Soc., 101–106.

National Climatic Data Center, 1985: *Storm Data.* Vol. 27, No. 5, 66 pp.

Perez, A. H., L. J. Wicker, and R. E. Orville, 1997: Characteristics of cloud-to-ground lightning associated with violent tornadoes. *Wea. Forecasting,* **12,** 428–437.

Reap, R. M., and D. R. MacGorman, 1989: Cloud-to-ground lightning: Climatological characteristics and relationships to model fields, radar observations, and severe local storms. *Mon. Wea. Rev.,* **117,** 518–534.

Rutledge, S. A., and D. R. MacGorman, 1988: Cloud-to-ground lightning activity in the 10–11 June 1985 mesoscale convective system observed during the Oklahoma–Kansas PRE-STORM project. *Mon. Wea. Rev.,* **116,** 1393–1408.

——, C. Lu, and D. R. MacGorman, 1990: Positive cloud-to-ground lightning in mesoscale convective systems. *J. Atmos. Sci.,* **47,** 2085–2100.

Saffle, R. E., 1977: A case study of reported severe weather events and concurrent vertically integrated liquid water content values. Preprints, *10th Conf. on Severe Local Storms,* Omaha, NE, Amer. Meteor. Soc., 104–109.

——, and R. C. Elvander, 1981: Use of digital radar in automated short range estimates of severe weather probabilities and radar reflectivity. Preprints, *Seventh Conf. on Probability and Statistics,* Monterey, CA, Amer. Meteor. Soc., 192–199.

Schuur, T. J., B. F. Smull, W. D. Rust, and T. C. Marshall, 1991: Electrical and kinematic structure of the stratiform precipitation region trailing an Oklahoma squall line. *J. Atmos. Sci.,* **48,** 825–842.

Stolzenburg, M., T. C. Marshall, W. D. Rust, and B. F. Smull, 1994: Horizontal distribution of electrical and meteorological conditions across the stratiform region of a mesoscale convective system. *Mon. Wea. Rev.,* **122,** 1777–1797.

——, W. D. Rust, B. F. Smull, and T. C. Marshall, 1998: Electrical structure in thunderstorm convective regions: 1. Mesoscale convective systems. *J. Geophys. Res.,* **103,** 14 059–14 078.

Watson, A. I., R. L. Holle, and R. E. López, 1995: Lightning from two national networks related to vertically integrated liquid and echo-top information from WSR-88D radar. *Wea. Forecasting,* **10,** 592–605.

Winston, H. A., and L. Ruthi, 1986: Evaluation of RADAP II severe-storm-detection algorithms. *Bull. Amer. Meteor. Soc.,* **67,** 145–150.